Cellulose (2010) 17:139–151
DOI 10.1007/s10570-009-9355-4

Structure elucidation of uniformly ^{13}C-labeled bacterial celluloses from different *Gluconacetobacter xylinus* strains

Stephanie Hesse-Ertelt · Thomas Heinze · Eiji Togawa · Tetsuo Kondo

Received: 17 March 2009 / Accepted: 9 August 2009 / Published online: 25 August 2009

Abstract The morphological and supramolecular structures of native cellulose pellicles from two strains of *Gluconacetobacter xylinus* (ATCC 53582, ATCC 23769) were investigated. Samples had been statically cultivated in Hestrin-Schramm medium containing fully ^{13}C-labeled β-D-glucose-U-$^{13}C_6$ as the sole source of carbon. The results are compared with structure data of bacterial celluloses with a natural ^{13}C abundance of 1.1%. Non-enriched and ^{13}C-labeled cellulose pellicles formed crystalline structures as revealed by cross-polarized/magic-angle spinning (CP/MAS) $^{13}C\{^1H\}$-NMR and near infrared (NIR) FT-Raman spectroscopic measurements as well as wide-angle X-ray diffraction (WAXD) investigations. Atomic force microscopy (AFM) was applied for analyzing fiber morphologies and surface properties. For the first time, details about the manipulation of fiber widths and pellicle formation were shown for different bacterial strains of *G. xylinus* depending on the use of β-D-glucose-U-$^{13}C_6$ for the biosynthesis.

Keywords Bacterial cellulose · *Gluconacetobacter xylinus* · ^{13}C-Labeling · Biosynthesis · ^{13}C Nuclear magnetic resonance · NIR FT-Raman · Atomic force microscopy · Wide-angle X-ray diffraction · Crystallinity

Abbreviations

A. xylinum	*Acetobacter xylinum*
AFM	Atomic force microscopy
ATCC	American type culture collection
AY-201	Bacterial strain ATCC 23769
BC	Bacterial cellulose
CI	Crystallinity index
CP	Cross polarization
DSM	Deutsche Sammlung von Mikroorganismen
FT-Raman	Fourier transformed Raman
FWHM	Full width at half maximum
G. xylinus	*Gluconacetobacter xylinus*
HS	Hestrin-Schramm
I_α, I_β	Cellulose modifications
I_c	Crystallinity value obtained by NMR
INADEQUATE	Incredible natural abundance double quantum transfer experiment

S. Hesse-Ertelt (✉) · T. Heinze
Friedrich Schiller University of Jena,
Centre of Excellence for Polysaccharide Research,
Humboldtstrasse 10, 07743 Jena, Germany
e-mail: stephanie.hesse@uni-jena.de

E. Togawa
Forestry and Forest Products Research Institute (FFPRI),
Matusnosato 1, Tsukuba, Ibaraki 305-8687, Japan

T. Kondo
Bio-Architecture Center (KBAC) and Graduate School of Bioresource and Bioenvironmental Sciences,
Kyushu University, 6-10-1 Hakozaki, Higashi-ku,
Fukuoka 812-8581, Japan

MAS	Magic angle spinning
NIR	Near infrared
NMR	Nuclear magnetic resonance
NOC	Nematic ordered cellulose
NQ-5	Bacterial strain ATCC 53582
TPPM	Two pulse phase modulation
WAXD	Wide-angle X-ray diffraction
x_c	Crystallinity value obtained by WAXD

Introduction

Cellulose possesses a large complexity and variability in its supramolecular arrangement and, depending on the conditions of its structure formation, displays a significant diversity in structural features such as lattice composition, crystallite dimensions, crystallinity, and fibrillar orientation (Ganster and Fink 1999; Klemm et al. 2005). Besides the monoclinic structure model (Meyer and Misch 1937) describing the allomorph I_β (space group: $P2_1$), a triclinic structure (Sarko and Muggli 1974) was defined for the native cellulose I, characterizing the allomorph I_α (space group: P1). As a model substance for the investigation of biosynthesis and crystallization of native cellulose, bacterial cellulose (BC) from *Gluconacetobacter xylinus* (previously referred to as *Acetobacter xylinum*) was used (Brown et al. 1976; Kuga and Brown 1991). Never-dried BC is a highly swollen biopolymer with approximately 99 wt.% of water (Fink et al. 1997), and was investigated in dependence on the drying conditions (Bohn 2000; Udhardt et al. 2005). It could be shown that the biosynthesis of cellulose macromolecules was connected with their self assembling. Caused by the drying procedure, the sizes of the cellulose crystallites decreased. Moreover, a uniplanar orientation value already resulted in the never-dried state. It was found that the (1–10) crystal lattice plane was parallel oriented to the macroscopic surface of the cellulose pellicle (Bohn et al. 2000). Formation and structure of BC can be controlled by varying the components of both nutrient medium and cultivation conditions (Klemm et al. 2001; Seifert et al. 2004), which sparks interest in fundamental investigations of the biosynthesis and microgravitative effects of the formation of cellulose by *G. xylinus*. Besides vibrational spectroscopy, which played an important role in the investigation of the molecular conformations and hydrogen bonding patterns of cellulose (Schenzel and Fischer 2001; Schenzel et al. 2005; Fischer et al. 2005), solid-state nuclear magnetic resonance (NMR) spectroscopy was widely used to study the structure of cellulose from different sources (Erata et al. 1997; Atalla and VanderHart 1999; Kono et al. 2002, 2003; Numata et al. 2003; Kono and Numata 2006). With regard to NMR investigations, the impact of the ^{13}C isotope in isotopically enriched samples is of particular interest. However, investigations on the ^{13}C-labeling are rarely described (Gagnaire and Taravel 1980; Arashida et al. 1993; Kai et al. 1994, 1998; Evans et al. 1996). Recent publications explain the finally received BC and the mechanism of labeling transfer from carbon to carbon. Further results are limited to cell movement- and cell division rates. In this regard, Kondo and co-workers found a cell movement rate on nematic ordered cellulose (NOC: Togawa and Kondo 1999; Kondo et al. 2001) of about 4.5 μm per min for *G. xylinus* ATCC 53582 in non-enriched nutrient media (Kondo et al. 2002). These results were confirmed later using *G. xylinus* ATCC 53582 and ATCC 23769 in different cultivation media and furthermore, the influence of a modified distribution of carbon isotopes on both biological systems and microgravitative effects of the cellulose building was proven using β-D-glucose-U-$^{13}C_6$ for the biosynthesis (Hesse and Kondo 2005). It was found that the bacterial strains divided faster in a ^{13}C-enriched than in common nutrient media, and the cell movement was influenced by the bacterial strain and by the carbon isotope distribution of the D-glucose used. On NOC, the movement of a single *G. xylinus* ATCC 53582 cell was decelerated by the ^{13}C-isotope to be only half the speed, while the movement of a single *G. xylinus* ATCC 23769 cell was less influenced. Caused by their different sizes, *G. xylinus* ATCC 23769 cells generally produce smaller cellulose microfibrils than *G. xylinus* ATCC 53582 cells. Nevertheless, the fiber structure of freshly biosynthesized and deposited cellulose nanofibers on the surface of NOC was proved to be in the crystalline state of cellulose I (Hesse and Kondo 2005). These studies are related to shaken cultures of *G. xylinus*. Continuing studies are concerned with the investigation of *G. xylinus* ATCC 53582 and ATCC 23769 in static culture. BC pellicles biosynthesized by these bacterial strains with β-D-glucose-U-$^{13}C_6$

were analyzed and compared with non-enriched samples. Previously, refined ^{13}C-NMR chemical shift data of the dominant cellulose I_α modification were obtained using 2D refocused INADEQUATE on ^{13}C-labeled BC pellicles (Hesse-Ertelt et al. 2008). Their respective isotropic ^{13}C chemical shifts exhibited only slight differences, but there were major discrepancies compared to the ^{13}C chemical shift data of BC from another *G. xylinus* strain (DSM 13368) grown at different cultivation conditions. Apparently, the structure of the crystalline allomorph I_α does not only depend on its origin (algae or bacterial cellulose, etc.), but also on the cultivation conditions and possibly on the type of bacterium used for biosynthesis.

Even though NMR spectroscopy just showed marginal differences for the non-enriched- and ^{13}C-labeled BC produced by the same strain of *G. xylinus*, further structural investigations of the cellulose pellicles are required. Since isotopically exchanged BC samples are notably used as model substances in solid-state NMR spectroscopy, it is necessary to know if they are representative of the corresponding natural celluloses. It should be ensured that the application of fully ^{13}C-labeled β-D-glucose-U-$^{13}C_6$ does not have any influence on the building of cellulose pellicles. In this work, the insight on the distinctive character of BC samples from different strains of *G. xylinus* discussed in (Hesse-Ertelt et al. 2008) are also confirmed by analytical methods other than solid-state NMR. Differences in the morphological and crystalline structures of the BC pellicles produced by *G. xylinus* ATCC 53582 and *G. xylinus* ATCC 23769 are described depending on their ^{13}C-labeling.

Experimental section

Bacterial cellulose

Two types of *G. xylinus* strains (NQ-5: ATCC 53582 of about 10 µm length, and AY-201: ATCC 23769 of about 2 µm length) were cultured in sterilized Hestrin-Schramm (HS) medium (Hestrin and Schramm 1954) at pH 6.0 using different kinds of carbon sources: β-D-glucose (^{13}C, 1.1%; Sigma–Aldrich Chemicals Co., USA) and uniformly ^{13}C-enriched β-D-glucose-U-$^{13}C_6$ (^{13}C, 99%; Campro Scientific, Germany and Sigma–Aldrich Chemicals Co. USA). For cultivation, 200 µL of preparatory cultures of the respective *G. xylinus* strains grown with β-D-glucose (^{13}C, 1.1%) were inoculated per 8.3 ml of autoclaved HS media. The culture media were incubated statically at 30 °C for a period of 14 days, during which the pre-polymer was not removed. After cultivation, the pellicles were washed with distilled water, treated with 0.1N aqueous NaOH solution at 80 °C for 4 h, and washed again with running water to a neutral reaction of the rinsing agent. Finally, the pellicles were air dried (covered by aluminum foil) at 50 °C for 24 h.

BC pellicles **1**–**3** were prepared using β-D-glucose (^{13}C, 1.1%) by *G. xylinus* ATCC 53582 (**1**) and *G. xylinus* ATCC 23769 (**2**, **3**). BC samples **4**–**6** were prepared using β-D-glucose-U-$^{13}C_6$ (^{13}C, 99%) by *G. xylinus* ATCC 53582 (**4**) and *G. xylinus* ATCC 23769 (**5**, **6**).

Atomic force microscopy

Samples were measured in the air dried state using SHIMADZU's SPM-9500J3. The AFM measurements were carried out in contact mode at a scan rate of 1 Hz using etched silicon tips with a cantilever spring constant of about 0.13 N.

Wide-angle X-ray diffraction

For WAXD measurements, samples were investigated in the air dried state using the RIGAKU X-ray diffractometer RINT-2500HF. CuK_α irradiation and transmission technique have been used at following conditions: 0.5°/min, $2\theta = 5\ldots60°$, 40 kV, and 200 mA, whereas step sizes of 0.02° were applied.

NIR FT-Raman spectroscopy

The samples were placed across the sample holders and measured in the air dried state using the Bruker Equinox 55 (FRA 106/S with D 418-T) spectrometer with a liquid-nitrogen cooled Ge diode as detector. A cw-Nd:YAG-laser operating at $\lambda_{Nd:YAG} = 1{,}064$ nm with a maximum power of 450 mW was used as light source for the excitation of the Raman scattering. The spectra have been detected over the range of 3,500–400 cm^{-1} using an operating spectral resolution of 4 cm^{-1} and averaged over 500 scans.

NMR spectroscopy

CP/MAS $^{13}C\{^{1}H\}$-NMR spectra were recorded on a Bruker AMX 400 MHz (AMX 400) spectrometer operating at 100.58 MHz for ^{13}C, with a 4 mm MAS double resonance probe and ZrO_2 rotors. The measurements were carried out at 6.5 kHz MAS. The cross polarization (CP) contact time was 1 ms; 64, 4 k, and 20 k scans were accumulated. Two-pulse phase modulation (TPPM: ±10°, 7 μs and 8 μs, respectively) was applied for proton decoupling. The recycle delay was set to 2 s for all experiments, and adamantane was used as an external reference having ^{13}C chemical shifts of 29.50 ± 0.10 ppm (CH) and 38.56 ± 0.10 ppm (CH_2) with respect to tetramethylsilane at 0.0 ppm (Earl and VanderHart 1982).

Results and discussion

Bacterial cellulose

To investigate the biosynthesis properties of *G. xylinus* NQ-5 and AY-201 as well as pellicle surfaces of their products, the subspecies of *G. xylinus* were biosynthesized in static culture. During the first incubation days, no significant differences in the cultivation behavior of both bacterial strains occurred. The microorganisms always produced gelatinous and transparent substances on the surface of the HS medium. Comparable to results of (Groebe et al. 1991), BC pellicles were able to bind high amount of water. Typically, these substances increasingly gained thickness and became turbid after about three incubation days. The maximum cellulose production could be observed after 6 days cultivation period. The slight shift in the incipient cellulose production with respect to the growth of cells was due to a limitation of nutrients in the HS medium. Thus, BC pellicles are considered as products of the secondary metabolism of cells. It was proven that the morphology of BC pellicles varied between different subspecies of *G. xylinus*, and the polydispersities were different for BC NQ-5 ($M_w/M_n = 2.82$) and BC AY-201 ($M_w/M_n = 5.69$). Furthermore, significant varieties in the pellicle formation occurred in the presence of β-D-glucose-U-$^{13}C_6$ (^{13}C, 99%) with respect to β-D-glucose (^{13}C, 1.1%).

BC NQ-5 was produced each with β-D-glucose (**1**) and with β-D-glucose-U-$^{13}C_6$ (**4**). Considering their sensitivity and associated risks of irregular pellicle formation, AY-201 (ATCC 23769) cells were used for the biosynthesis of two different batches of non-enriched (**2**, **3**) and ^{13}C-labeled BC (**5**, **6**). For both batches, the simultaneous synthesis of non-enriched BC NQ-5 served as reference (R^1, R^2). Reference samples were prepared independently from the batch of BC NQ-5 (**1**, **4**), just for the purpose of comparison with sample **1**. R^1 and R^2 were biosynthesized using the same non-enriched nutrient media as used for the synthesis of the corresponding BC AY-201 (**2**, **3**).

Thicknesses and weights of the biosynthesized BC pellicles were analyzed. Each sample was weighted again after air-drying. Table 1 shows results of the never-dried BC pellicles (thicknesses d_p) and after sample drying (weights m_a, fiber widths d_f).

1. In case of BC NQ-5, the pellicle formation proceeded uniformly for the non-enriched and ^{13}C-labeled samples. The averaged pellicle thicknesses varied at about 0.7 mm. However, the part of the produced dry mass of ^{13}C-labeled BC (**4**, $m_a \approx 17$ mg) was obviously higher than that of conventional BC NQ-5 (**1**, $m_a \approx 13$ mg). The pellicle growths of the reference samples R^1 and R^2 occurred homogeneously as well, although their dry masses were slightly lower ($m_a \approx$ 12 mg) than that of sample **1**.
2. In contrast, the first batch of BC AY-201 (BC AY-201^1: **2**, **5**) showed an inhomogeneous growth of pellicles. After five incubation days, a stagnancy of growth was observed for the non-enriched BC **2** at about 2.5 mm pellicle thickness, whereas the AY-201 cells already produced more than twice the number ($d_p \approx 6$ mm) of ^{13}C-labeled BC (**5**) in the same time. Pellicle thicknesses and -weights of **2** and **5** were significantly different. This fact permits several explanations. The cellulose production of non-enriched samples was obviously affected, which might be due to impurities of the nutrient medium. Qualitative differences in the HS medium could also explain the lower mass of R^1 compared to BC **1**. Furthermore, it could be possible that AY-201 cells were able to metabolize the ^{13}C-labeled β-D-glucose-U-$^{13}C_6$ more efficiently than β-D-glucose.

Table 1 Averaged pellicle thicknesses (mm), -weights (mg), and fiber widths (nm) of bacterial celluloses biosynthesized by *G. xylinus* strains

			Pellicle thicknesses[a] d_p (mm)	Pellicle weights[a] m_a (mg)	Fiber widths[a] d_f (nm)
	R^1	Reference BC NQ-5	5.8	11.7	–/–
	R^2		6.8	11.8	–/–
β-D-glucose (^{13}C, 1.1%)	1	BC NQ-5	7.0	13.1	81.1
	2	BC AY-201[b]	2.5	3.6	59.0
	3	BC AY-201[c]	10.5	5.7	60.0
β-D-glucose-U-$^{13}C_6$ (^{13}C, 99%)	4	BC NQ-5	7.7	16.9	67.4
	5	BC AY-201[b]	6.2	6.8	59.2
	6	BC AY-201[c]	10.8	6.6	60.5

R^1/R^2 reference BC of the two batches of BC AY-201

[a] Standard deviations turned out to be 0.5 mm (thicknesses), 0.8 mg (weights), and 1 nm (widths); fiber widths were obtained by 25 single measurements per BC pellicle using AFM

[b] First batch of BC AY-201 (**2**, **5**)

[c] Retry (**3**, **6**)

3. Hence, a second batch of BC AY-201 (BC AY-201^2: **3**, **6**) was produced for verification, exhibiting pellicles of almost the same thicknesses ($d_p \approx 11$ mm), cf. Table 1. However, the weights of the air-dried samples still varied to about 1 mg between non-enriched (**3**) and ^{13}C-labeled BC AY-201 (**6**). Extremely different thicknesses were measured for the two ^{13}C-enriched pellicles of BC AY-201 (**5**, **6**), but their weights in the air-dried state were identical ($m_a \approx 7$ mg). This fact suggests that AY-201 cells were able to include high and different amount of water in the same mass of cellulose pellicles. Since the nutrient media of both batches were not varied, the process of water retention was irregular and obviously uncontrollable.

In each case, however, a deceleration of pellicle growth was observed with increasing time of incubation. This fact might be due to the limitation and a non-warranted supply of nutrients in the HS medium. The partial pressure of O_2 decreased for instance with increasing film thickness. Active bacteria were just found in a subsurface band of 1 mm size. Furthermore, the concentration of β-D-glucose decreased with longer incubation time, which was independent from the ^{13}C-labeling. The glucose was completely metabolized in the aerobic surface area after about 15 days.

Finally, it was shown that non-enriched samples of BC NQ-5 and BC AY-201 were always of lower mass than the ^{13}C-enriched ones of the same batches. Thus, β-D-glucose-U-$^{13}C_6$ (^{13}C, 99%) seemed to enhance the cellulose production.

Atomic force microscopy

The widths of cellulose fibers from common and ^{13}C-enriched BC pellicles were determined by atomic force microscopy (AFM) for further quantitative information. Different ranges have been scanned for both subspecies of *G. xylinus* (Fig. 1).

It was found that a scan range of 5 × 5 μm was optimum for quantitative analyses. AFM measurements have been carried out at five different scan ranges for each sample. The fiber widths could be determined by SPM-9500J3 software, at which five fibers per measurement were analyzed for each sample. The results were averaged with a standard deviation of about 1 nm.

Even though drastic differences occurred in their thicknesses and weights, the fiber widths of BC AY-201 were almost constant for ^{13}C-labeled- and non-enriched pellicles, cf. Table 1. In contrast, the averaged fiber width of BC NQ-5 decreased by 14 nm (17%) from 81 nm to about 67 nm using β-D-glucose-U-$^{13}C_6$ (^{13}C, 99%) for the biosynthesis. Pellicle thicknesses and -weights (Table 1), however, suggested that NQ-5 cells prefer metabolizing ^{13}C-labeled β-D-glucose. Considering the smaller fiber widths of ^{13}C-enriched BC NQ-5 in combination with

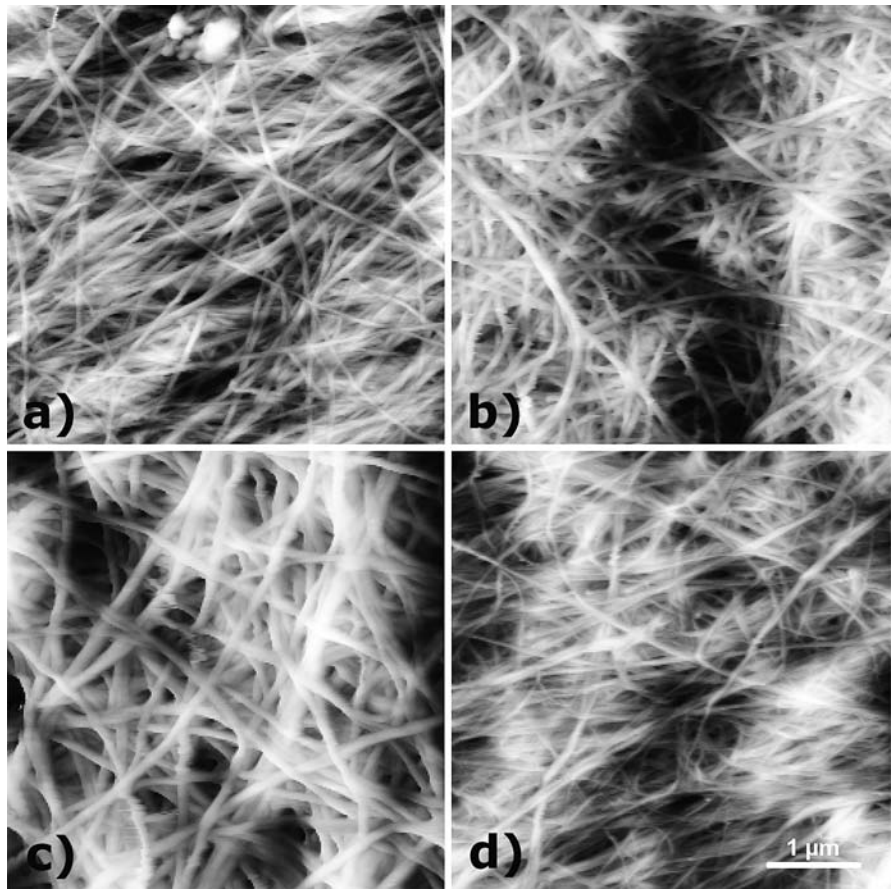

Fig. 1 AFM topographies (5 × 5 µm) of bacterial celluloses produced by different *G. xylinus* strains in different culture media: **a** common BC AY-201[2] (**3**), **b** ^{13}C-enriched BC AY-201[2] (**6**), **c** common BC NQ-5 (**1**), and **d** ^{13}C-enriched BC NQ-5 (**4**)

slower cell movement on templates and higher cell division rates of *G. xylinus* NQ-5 in ^{13}C-enriched HS media (Hesse and Kondo 2005), β-D-glucose-U-$^{13}C_6$ (^{13}C, 99%) seemed to stimulate the cell division only.

Consequently, more NQ-5 bacteria produced a larger quantity of cellulose with averaged smaller fiber widths in the presence of the ^{13}C-isotope in the same time. In comparison, AY-201 bacteria were also swayed by the ^{13}C-labeling of the carbon source, but they were more susceptible to least modifications of the HS medium and/or cultivation conditions.

Wide-angle X-ray diffraction

The parameters of the supermolecular structure of BC pellicles like crystallite sizes and orientations were determined by wide-angle X-ray diffraction (WAXD) measurements. In this work, the convention of (Sarko and Muggli 1974) was used for the description of BC. Figure 2 and 3 show that, in general, each of the typical reflections of cellulose I could be found.

Usually, the (110) crystal lattice planes describe the orientation of crystallites to the sample surface. In case of BC NQ-5 (**1**, **4**), the reflections qualitatively pointed out a crystalline cellulose modification I of high degree of order (Fig. 2). Figure 3 shows WAXD curves of BC AY-201 (**2**, **3**, **5**, and **6**); here, an additional interference at $2\Theta = 12.6°$ was detected for sample **2**, which was not typical for native cellulose of modification I. It could be assigned to the (1-10) crystal lattice plane of cellulose II indicating a change in the cellulose polymorphs of BC AY-201[1] (**2**). However, sample **2** was characterized by a high planar orientation. It was confirmed previously that the typical structure of cellulose produced by wild-type ATCC 23769 cells was a twisting ribbon of cellulose I and furthermore, a small quantity of anomalous material. This band material composed of cellulose II was recognized by careful examination (Brown et al. 1976; Brown 1989; Kuga et al. 1993). A continuative phenomenon was found by (Hirai et al. 1997). They stated that the same cell of ATCC 23769

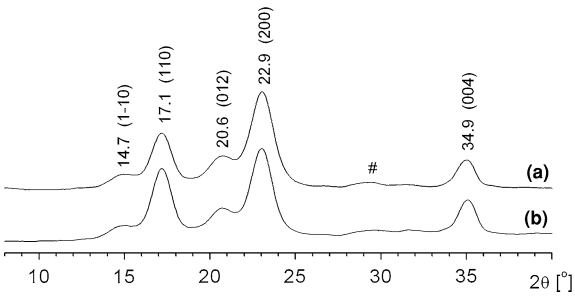

Fig. 2 WAXD curves of bacterial cellulose pellicles of the strain *G. xylinus* NQ-5 that were biosynthesized **a** In ^{13}C-enriched culture liquid (**4**) and **b** In common HS medium (**1**); # meridian interferences

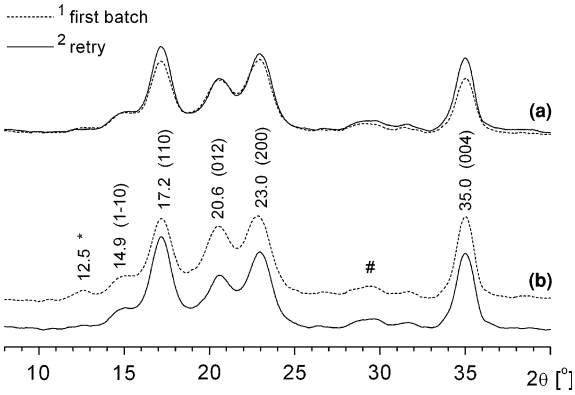

Fig. 3 WAXD curves of bacterial cellulose pellicles of the strain *G. xylinus* AY-201 that were biosynthesized **a** In ^{13}C-enriched culture liquid (**5**, **6**) and **b** In common HS medium (**2**, **3**). # meridian interferences; * reflex of the (1–10) plane of cellulose II. [1]first batch of BC AY-201 (**2**, **5**), [2]retry (**3**, **6**)

can produce cellulose I and II depending on the culture temperature. Thus, the bacterium AY-201 seems to be readily manipulable. Cellulose produced by these cells possibly consists of a compound of cellulose modification I and II meaning that the cultivation conditions widely influenced the amount of biosynthesized cellulose II by the bacterium.

Additionally, the first batch of BC AY-201 (**2**, **5**) exhibited the abort of pellicle's growth in common HS media after 5 days incubation time, whereas β-D-glucose-U-$^{13}C_6$ (^{13}C, 99%) forced bacteria to keep on biosynthesizing cellulose. Finally, the two ^{13}C-enriched pellicles of BC AY-201 (**5**, **6**) were twice as thick as pellicles grown in common HS media (**2**, **3**), cf. Table 1. Moreover, their WAXD curves diverge. Neither for the ^{13}C-labeled BC of the first batch nor for the ^{13}C-enriched one of the retry, such an intensive reflex was detected at 12.6° as for the non-enriched pellicle of the first batch of BC AY-201 (**2**). Crystal lattice planes, wide angle 2Θ, and distance d of this sample were given in cursive characters in Table 2. All of the other data were averaged.

To analyse WAXD curves, the crystallite index CI was determined according to (Jayme and Knolle 1964) using Eq. 1. Their method is mainly based on investigations of (Hermans and Weidinger 1946) and (Kast and Flaschner 1948).

$$\mathrm{CI} = \frac{F_c}{F_c + F_a} \tag{1}$$

The CI values of the WAXD intensity curves were determined using integral values of crystalline and non-crystalline regions obtained by ORIGIN PEAK FITTING. Results of five measurements were averaged; the maximum standard deviation is 0.01.

Crystallinity values between 64.4 and 66.5% were determined. However, there was almost no difference between pellicles of the different *G. xylinus* strains nor of different ^{13}C-percentage. BC NQ-5 (**1**, **4**) exhibited more crystalline parts than pellicles of BC AY-201; and in each case, the crystallinity values decreased marginally by ^{13}C-enrichment. These results correlate with CP/MAS ^{13}C{^{1}H}-NMR data.

Generally, Bragg reflections cannot be sharpened randomly, they were broadened. This fact was described quantitatively by Δ(2Θ), the full width at half maximum (FWHM), of the observed reflections that have FWHM as a function of the wide angle 2Θ. The experimentally obtained FWHM values of the respective line positions were caused by the finite grading of the tested powder and were inversely correlated to the crystallite sizes. The FWHM values increased with decreasing number of the involved crystal lattice planes. The crystallite dimensions of the equatorial and meridional wide-angle interferences could be calculated from the size-depending increment of the FWHM values using the formula of Scherrer 2. It should be noted that FWHM values were falsified by crystal lattice defects, broad grain size distributions, and instrumental peak broadening. Thus, experimentally determined crystallite sizes should refer to as averaged minimum crystallite dimensions. In case of cellulose, the deviation from

Table 2 Averaged crystallite indices CI, crystallinities x_c (%), wide angles 2Θ, full widths at half maximum Δ(2Θ), crystallite sizes D_{hkl} (nm) and distances d (nm) of bacterial cellulose pellicles produced by *G. xylinus* strains

Lattice plane			Bacterial cellulose from *G. xylinus* ATCC 53582 (NQ-5)							
			Natural ^{13}C abundance (1.1%) (CI = 0.665, x_c = 66.5%)				Uniformly ^{13}C-labeled (94%) (CI = 0.651, x_c = 65.1%)			
			2Θ (°)	Δ(2Θ)	D_{hkl} (nm)	d (nm)	2Θ (°)	Δ(2Θ)	D_{hkl} (nm)	d (nm)
1	−1	0	14.7	0.741	10.7	0.604	14.6	0.741	10.7	0.605
1	1	0	17.1	1.231	6.5	0.517	17.1	1.330	6.0	0.518
0	1	2	20.6	0.769	10.4	0.431	20.6	0.612	13.1	0.432
2	0	0	22.9	1.404	5.7	0.387	22.9	1.365	5.9	0.388
0	0	4	35.0	1.263	6.5	0.256	34.9	1.212	6.8	0.257
Lattice plane			Bacterial cellulose from *G. xylinus* ATCC 23769 (AY-201)							
			Natural ^{13}C abundance (1.1%) (CI = 0.657, x_c = 65.7%)				Uniformly ^{13}C-labeled (94%) (CI = 0.644, x_c = 64.4%)			
			2Θ (°)	Δ(2Θ)	D_{hkl} (nm)	d (nm)	2Θ (°)	Δ(2Θ)	D_{hkl} (nm)	d (nm)
1	*−1*	*0*	*12.6*	*–/–*	*–/–*	*0.700*	*–/–*	*–/–*	*–/–*	*–/–*
1	−1	0	15.0	–/–	–/–	0.591	15.0	–/–	–/–	0.590
1	1	0	17.2	1.275	6.2	0.515	17.2	1.271	6.3	0.516
0	1	2	20.6	1.299	6.2	0.432	20.5	1.365	5.9	0.431
2	0	0	23.0	1.440	5.6	0.387	23.0	1.482	5.4	0.387
0	0	4	35.0	1.247	6.6	0.256	35.0	1.259	6.5	0.256

BC NQ-5: samples **1**, **4**, R^1, and R^2 were investigated; BC AY-201: samples **2**, **5**, **3**, and **6** were investigated. *Cursive values:* sample **2** (BC AY-201^1)

the actual crystallite dimensions should be less than 10% (Fink and Walenta 1994; Fink et al. 1995).

$$\Delta(2\Theta)^* = \frac{k \cdot \lambda}{D_{hkl} \cdot \cos(\Theta)} \quad (2)$$

The parameters of Equation 2 were defined as follows: D_{hkl} = crystallite size $\gg \lambda$, k = 0.89, $\Delta(2\Theta)^*$ = FWHM-increment, λ = wavelength of CuK_α-irradiation, and 2Θ = wide angle. It should be mentioned that $\Delta(2\Theta)^*$ just describes an increment of FWHM that contains an equipment-sourced part besides the actually resulting FWHM value Δ(2Θ) from the experiment. The parameter variation, depending on the X-ray diffraction equipment, was not included in the calculations.

Independent from the ^{13}C-enrichment, the crystallite sizes of BC averaged out to be 5–7 nm for both, BC NQ-5 and BC AY-201 with the exception of the (012) crystal lattice plane of BC NQ-5 (**1**, **4**). Here, crystallite sizes turned out to be $D_{hkl\varnothing} \approx 12$ nm for the non-enriched and ^{13}C-labeled samples. No remarkable difference between common BC pellicles and BC grown on the ^{13}C isotope was found.

NIR FT-Raman spectroscopy

Previously, it was published that NIR FT-Raman spectra of 3 days old cellulose fibers produced by *G. xylinus* NQ-5 in shaken cultures clearly proved the polymorphic state of cellulose I (Hesse and Kondo 2005).

In this work, NIR FT-Raman spectra demonstrated the vibrational behavior of BC NQ-5- and BC AY-201 pellicles depending on the polymorphic state of cellulose. The assignment of vibrational modes was derived from literature (Blackwell et al. 1970; Atalla 1976; Wiley and Atalla 1987). Our focus was simply directed towards the vibrational modes in the conformational sensitive range below 1,500 cm^{-1} that were favorable for characterizing polymorphic changes. The cross-denoted wave numbers of the NIR FT-Raman spectra of BC pellicles (BC NQ-5: **1**, **4**; BC AY-201^2: **3**, **6**) in Fig. 4 clearly indicated vibrational frequencies, which characterized the crystalline phase of cellulose I. Similar results were obtained for BC AY-201^1 (**2**, **5**—without illustration).

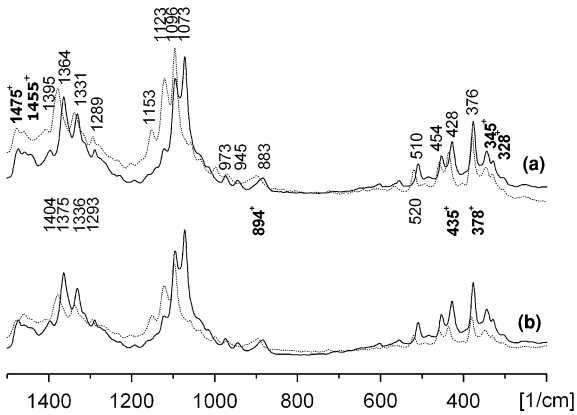

Fig. 4 NIR FT-Raman spectra of **a** BC NQ-5 pellicles (**1**: *dots*; **4**: *line*), and **b** BC AY-201[2] pellicles (**3**: *dots*; **6**: *line*) in the range of 1,500–200 cm^{-1}; $^{+}$Cellulose I-typical wave numbers

The internal coordinates of the frequency range of 1,500–800 cm^{-1} were due to modes involving considerable couplings of methine bending, methylene rocking and wagging, and COH in-plane bending vibrations. Except for the internal modes of the CH_2OH groups, all motions were completely delocalized. The results of the NIR FT-Raman spectra of samples **1**–**6** were in good agreement with data of BC published by (Schenzel and Fischer 2001), even though just medium-weak intensity bands could be detected below 1,400 cm^{-1} compared with the band at 1,452 cm^{-1}. Interestingly, the NIR FT-Raman band at 895 cm^{-1}, which was inversely correlated with the lateral size of the cellulose crystallites (Wiley and Atalla 1987), possessed a very low intensity. ^{13}C-NMR experiments of native celluloses suggested that the intensity of this band is proportional to the amount of disorder in cellulose (VanderHart & Atalla 1984). Accordingly, the weak NIR FT-Raman band at 895 cm^{-1} was an indication of the high order of crystalline state of the biosynthesized cellulose pellicles. The vibrational spectrum of BC in the range of skeletal deformations was characterized by typical Raman peaks: 435, 378, 345 and 328 cm^{-1}.

It is worth mentioning that in the range of 420-1,400 cm^{-1}, the modes of ^{13}C-enriched BC of both *G. xylinus* strains (**4**–**6**) were shifted to smaller wave numbers compared to the respective bands of common BC (**1**–**3**), cf. Fig. 4. This fact indicated differences in the vibrational behavior of non-enriched and ^{13}C-labeled samples, even though the cellulose I-typical peaks were almost identical. In case of ^{13}C-labeled (**4**–**6**) and non-enriched (**1**–**3**) BC pellicles, remarkable differences appeared in the range of 1,160-1,050 cm^{-1} for the vibrational modes known as $\nu(COC)_{glycosidic;\ ring\ breathing,\ symmetric}$, $\nu(CC)_{ring\ breathing,\ asymmetric}$, and $\nu(CO)_{ring\ breathing,\ asymmetric}$, whose frequency distribution is sensitive to the orientation of the glycosidic linkage, and the asymmetric breathing of the anhydroglucose ring.

NMR spectroscopy

Previously, CP/MAS $^{13}C\{^{1}H\}$-NMR measurements were carried out on freshly biosynthesized and deposited cellulose nanofibers on nematic ordered cellulose templates. It could be shown that BC nanofibers were of crystalline state similar to the polymorphic state of common BC (Hesse and Kondo 2005). In addition, ^{13}C chemical shift data of non-enriched, never-dried pellicles of BC NQ-5 (**1**; before air-drying) and BC AY-201[2] (**3**; before air-drying) were given and furthermore, refined data of the dominant modification I_α were obtained for the uniformly ^{13}C-labeled BC **4** and **6** using 2D refocused INADEQUATE (Hesse-Ertelt et al. 2008).

In this work, pellicles of BC NQ-5 (**1**, **4**) and BC AY-201 (**2**, **3**, **5**, and **6**) were investigated in the air-dried state. Slight variations between the commonly produced bacterial celluloses **1**–**3** (Fig. 5b) and BC

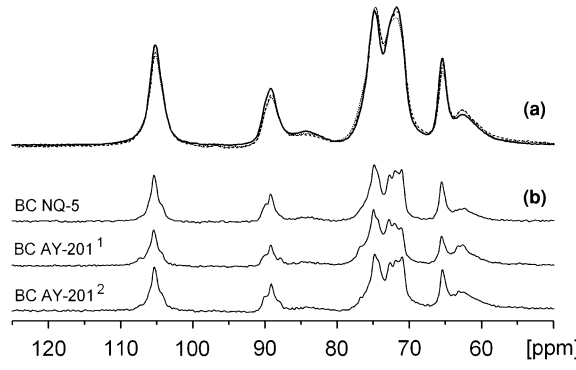

Fig. 5 CP/MAS $^{13}C\{^{1}H\}$-NMR spectra [AMX-400, 4 mm, $\nu_R = 6.5$ kHz, ns = 64, $t_w = 2$ s, $t_{CP} = 1$ ms, TPPM: ± 10°, 8 μs] of air-dried pellicles of **a** ^{13}C-enriched bacterial celluloses produced by *G. xylinus* NQ-5 (**4**: *line*) and *G. xylinus* AY-201 (**5**: *dots*; **6**: *dashes*), and of **b** commonly produced BC of the same strains (**1–3**) [ns = 4 k]

4–6, grown on the ^{13}C-isotope, (Fig. 5a) could be proved. Furthermore, differences in the NMR spectra of the two batches of BC AY-201 occurred.

Figure 5a shows CP/MAS ^{13}C{^{1}H}-NMR spectra of uniformly ^{13}C-labeled BC samples **4–6**. The samples were called BC NQ-5 (**4**; line), BC AY-201[1] (**5**; dots), and BC AY-201[2] (**6**; dashes). The data show that the ^{13}C-enrichment of samples **4-6** was successful with about 94% yield, virtually uniformly at all carbon positions. Compared to CP/MAS ^{13}C{^{1}H}-NMR spectra of non-enriched BC, the line shape characteristics and spectral resolution of the three fully ^{13}C-labeled samples in Fig. 5a were rather limited because of the strong homonuclear dipolar carbon–carbon couplings. Nevertheless, line shape analysis allowed the assignment of all ^{13}C chemical shifts of samples **4–6** on the basis of values of non-enriched BC (Hesse-Ertelt et al. 2008). There was no significant shift in their isotropic values.

As aforementioned, Fig. 5b shows CP/MAS ^{13}C{^{1}H}-NMR spectra of the non-enriched samples **1–3**. At first view, spectra exhibited typical resonances of cellulose modification I. However, varieties were observed for the different subspecies of *G. xylinus*. Comparing the non-enriched pellicles of BC AY-201[1] (**2**) and BC AY-201[2] (**3**), slight differences in the spectral line shapes became apparent. In case of BC **2**, additional parts could be detected, cf. Fig. 5b. The consideration of these additional parts was necessary for further analysis of sample **2**. Contrary to BC **2**, no indication of structural changes was observed for the respective ^{13}C-labeled sample in Fig. 5a, which might be due to the line broadening of the CP/MAS ^{13}C{^{1}H}-NMR spectra.

The CP/MAS ^{13}C{^{1}H}-NMR spectra of non-enriched, never-dried pellicles of BC NQ-5 (**1**; before air-drying) and BC AY-201[1] (**2**; before air-drying) were used for exact assignment, cf. Fig. 6. The ^{13}C chemical shifts of each BC could be readily assigned by line shape analysis taking into account data from the literature, e.g. (Kono et al. 2003). The fact that the chains in cellulose I_α are constructed by $-A_1-A_2-$ β-D-glucopyranose repeating units, while cellulose I_β is composed of two independent chains –B–B– and –B′–B′– (Kono and Numata 2006), was fully consistent with NMR data obtained. Caused by the excellent spectral resolution of the never-dried samples, CP/MAS ^{13}C{^{1}H}-NMR spectra were easily investigated by line shape analysis, cf. (Hesse-Ertelt et al. 2008). In case of BC AY-201[1] (**2**; before air-drying) an assignment was exclusively possible taking into account ^{13}C chemical shift data of other crystalline modifications of cellulose. Resonances at 107.4 and 76.8 ppm could be assigned to the $C1_1$ and $C3_2$ carbons of cellulose II, which might be a attributed to conformational changes of the BC AY-201[1] (**2**). Moreover, Fig. 6a showed peaks at 87.8 ppm and between 63 and 64 ppm corresponding to carbons of cellulose II, meaning that sample **2** consists of different cellulose modifications. These results were consistent with WAXD data. It should be mentioned that additional resonances could not be observed for BC AY-201 of the retry preparation (**3**). The ^{13}C-chemical shifts of pellicle **3** were in good agreement with data of BC NQ-5 (**1**) and each of the reference samples (R^1, R^2), respectively. By means of line shape analysis, the cellulose I-type with a high content of the I_α-allomorph could also be proved for the pellicles of BC NQ-5 (**4**) and BC AY-201 (**5**, **6**) biosynthesized in HS medium containing β-D-glucose-U-$^{13}C_6$ (I_α:$I_\beta \approx 2.5$:1).

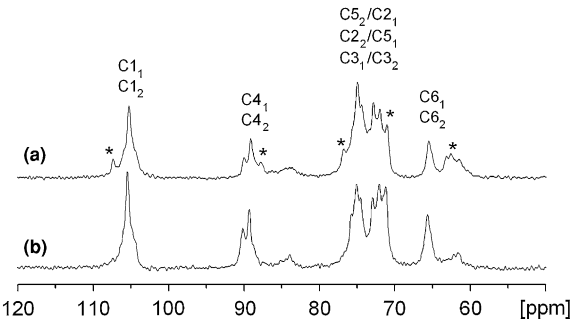

Fig. 6 CP/MAS ^{13}C{^{1}H}-NMR spectra [AMX-400, 4 mm, $\nu_R = 6.5$ kHz, $t_w = 2$ s, $t_{CP} = 1$ ms, ns = 20 k, TPPM: ± 10°, 7 µs] of non-enriched BC pellicles produced by **a** *G. xylinus* AY-201 (**2**; before air-drying) and **b** *G. xylinus* NQ-5 (**1**; before air-drying); *signs of an incipient change of the cellulose structure

Crystalline parts I_c (%) and I_α/I_β ratios of the several BC samples obtained by line shape analysis were summarized in Table 3. Basically, it could be shown in Fig. 5a that ^{13}C-labeled BC from *G. xylinus* ATCC 53582 and ATCC 23769 were of high crystallinity. As for the commonly produced BC NQ-5 (**1**), the quantitative analysis of the C4 resonances of the crystalline (~90 ppm) and amorphous (~84 ppm) components indicated that only about one-fourth of the ^{13}C-labeled BC NQ-5 (**4**) occurred

Table 3 Quantitative signal analysis of the CP/MAS $^{13}C\{^1H\}$-NMR spectra (Fig. 5)

	Natural ^{13}C abundance (1.1%)			Uniformly ^{13}C-labeled (94%)		
	BC NQ-5 1	BC AY-201[a] 2	BC AY-201[b] 3	BC NQ-5 4	BC AY-201[a] 5	BC AY-201[b] 6
I_α:I_β	2.7:1	2.2:1	2.7:1	2.6:1	2.4:1	2.5:1
I_c (%)	71	67	72	69	67	69
x_c (%)	67	−/−	66	65	−/−	64

Determination of the ratio I_α:I_β and the crystalline rates I_c (%) by line shape analysis of the C1 and C4 resonances

[a] First batch of BC AY-201 (**2**, **5**)

[b] Retry (**3**, **6**)

in non-crystalline regions. Comparable results were obtained for both batches of the ^{13}C-labeled BC AY-201 (**5**, **6**).<Dummy RefID="Tab3

In principle, the crystallinity values determined by ^{13}C-NMR spectroscopy ($I_c = 67\ldots71\%$) were marginally higher than the WAXD data obtained ($x_c = 64.4\ldots66.5\%$). Crystallinities of about 70% and the ratio of the crystalline modifications (I_α:$I_\beta \approx 2.6$:1) were similar to data from e.g. (Watanabe et al. 1998) and comparable to the values of never-dried BC from *G. xylinus* DSM 14666 (Hesse and Jaeger 2005), even though CP/MAS $^{13}C\{^1H\}$-NMR spectra of non-enriched BC AY-201 (**2**) indicated structural changes and the simultaneous existence of cellulose I- and II-type.

Conclusion

It was shown that β-D-glucose-U-$^{13}C_6$ (^{13}C, 99%) possibly enhanced the cellulose production of *G. xylinus* ATCC 53582 (NQ-5) and ATCC 23769 (AY-201) depending on the cell type. Usually, non-enriched samples of BC NQ-5 and BC AY-201 were of lower mass than the ^{13}C-enriched ones of the same batches. No differences could be found in fiber widths of BC AY-201 pellicles, while the averaged fiber width of BC NQ-5 decreased by 17% using β-D-glucose-U-$^{13}C_6$ (^{13}C, 99%) for the biosynthesis. Thus, NQ-5 bacteria produced a larger quantity of averaged smaller fibers in the presence of the ^{13}C-isotope, meaning that β-D-glucose-U-$^{13}C_6$ (^{13}C, 99%) stimulated the cell division. This fact is in agreement with previous results (Hesse and Kondo 2005). Using NIR FT-Raman spectroscopy, further differences in the vibrational behavior of non-enriched and ^{13}C-labeled samples of *G. xylinus* NQ-5 and AY-201 occurred, even though the cellulose I-typical peaks were almost identical. For the non-enriched and ^{13}C-labeled material, remarkable differences appeared for the skeletal stretching vibrations ν(COC), whose frequency distribution is sensitive to the orientation of the glycosidic linkage, and the asymmetric breathing of the anhydroglucose ring known as ν(CC) and ν(CO) vibrations. For BC NQ-5 and BC AY-201, the crystallite sizes of pellicles averaged out to be 5–12 nm independent from the ^{13}C-enrichment of the samples. Crystallinities of about 70% found by ^{13}C-NMR were marginally greater than the WAXD data, however, no remarkable differences between common BC and BC pellicles grown on the ^{13}C isotope were found by WAXD- and NMR-investigations. The ratio of the crystalline modifications (I_α:$I_\beta \approx 2.6$:1) was comparable to the values of never-dried BC from *G. xylinus* DSM 14666 (Hesse and Jaeger 2005), even though CP/MAS $^{13}C\{^1H\}$-NMR spectra of the non-enriched BC AY-201 indicated conformational changes. It should be mentioned that strong fluctuations in the pellicle formation of BC AY-201 occurred, due to inconsistent water retention. In summary, the use of ^{13}C-labeled D-glucose can lead to changes in the nature of the cellulose that might not be detectable by NMR- or WAXD-, but using NIR FT-Raman and AFM investigations. Consequently, some degree of caution is required, even using ^{13}C-enriched material as standard model in solid-state NMR.

Acknowledgments This research was financial supported by the Friedrich Schiller University of Jena (*Foerderung von Frauen in Forschung und Lehre*, Kapitel 1524/TG 84, 2002) for StHE, by MAFF Nanotechnology Project, Ministry of Agriculture, Forestry and Fisheries, and partly by a Grant-in-Aid for Scientific Research (No. 14360101), Japan Society for the Promotion of Science (JSPS) for TK. The authors are also indebted to Dr. U. Sternberg (FZ Karlsruhe, Germany) for partly financing D-glucose-U-$^{13}C_6$.

We thank Dr. S. Kimura and Ms. A. Morohoshi (FFPRI Tsukuba, Japan) for their kind assistance through this research, and Dr. W. Plass and Dr. A. Pohlmann (IAAC, FSU Jena, Germany) for providing the NIR FT-Raman spectrometer. StHE particularly thanks TK for the chance of sample preparation and characterization with his former group at the Forestry and Forest Products Research Institute (FFPRI), Matusnosato 1, Tsukuba, Ibaraki 305-8687, Japan.

References

Arashida T, Ishino T, Kai A, Hatanaka K, Akaike T, Matsuzaki K, Kaneko Y, Mimura T (1993) Biosynthesis of cellulose from culture media containing ^{13}C-labeled glucose as a carbon source. J Carbohydr Chem 12:641–649

Atalla RH (1976) Raman spectral studies of polymorphy in cellulose. Part I: Celluloses I and II. Appl Polym Symp 28:659–669

Atalla RH, VanderHart DL (1999) The role of solid state ^{13}C NMR spectroscopy in studies of the nature of native celluloses. Solid State Nucl Magn Reson 15:1–19

Blackwell J, Vasko PD, Koenig JL (1970) Infrared and Raman spectra of the cellulose from the cell wall of *Valonia ventricosa*. J Appl Phys 41:4375–4379

Bohn A (2000) Röntgenuntersuchungen zur Vorzugsorientierung und übermolekularen Struktur nativer und regenerierter Cellulose. Dissertation, TU Berlin

Bohn A, Fink HP, Ganster J, Pinnow M (2000) X-ray texture investigations of bacterial cellulose. Macromol Chem Phys 201:1913–1921

Brown RM Jr (1989) Cellulose biogenesis and a decade of progress: a personal perspective. In: Schuerch C (ed) Cellulose and wood: chemistry and technology. John Wiley and Sons, New York, pp 639–657

Brown RM Jr, Willison JHM, Richardson CL (1976) Cellulose biosynthesis in *Acetobacter xylinum*: visualization of the site of synthesis and direct measurement of the in vivo process. Proc Natl Acad Sci USA 73:4565–4569

Earl WL, VanderHart DL (1982) Measurement of ^{13}C chemical shifts in solids. J Magn Reson 48:35–54

Erata T, Shikano T, Yunoki S, Takai M (1997) The complete assignment of the ^{13}C CP/MAS NMR spectrum of native cellulose by using ^{13}C labeled glucose. Cellulose Commun 4:128–131

Evans RJ, Wang D, Agblevor FA, Chum HL, Baldwin SD (1996) Mass spectrometric studies of the thermal decomposition of carbohydrates using ^{13}C-labeled cellulose and glucose. Carbohydr Res 281(2):219–235

Fink HP, Walenta E (1994) Models of cellulose structure from the viewpoint of the cellulose I → II transition. Papier 12:739–748

Fink HP, Hofmann D, Philipp B (1995) Some aspects of lateral chain order in cellulosics from X-ray scattering. Cellulose 2:51–70

Fink HP, Purz HJ, Bohn A, Kunze J (1997) Investigation of the supramolecular structure of never dried bacterial cellulose. Macromol Symp 120:207–217

Fischer S, Schenzel K, Fischer K, Diepenbrock W (2005) Applications of FT Raman spectroscopy and micro spectroscopy characterizing cellulose and cellulosic biomaterials. Macromol Symp 223:41–56

Gagnaire D, Taravel FR (1980) Biosynthèse de cellulose bactérienne à partir de D-glucose uniformément enrichi en ^{13}C. Eur Biochem 103:133–143

Ganster J, Fink HP (1999) Physical constants of cellulose. In: Immergut EH, Grulke EA (eds) Polymer handbook, 4th edn. Wiley, New York, p V/135ff

Groebe A, Chmiel H, Strathmann H (1991) Verfahren zur Herstellung von Cellulose-Membranen aus bakteriell erzeugter Cellulose. EU Patent No. 0416470A2

Hermans PH, Weidinger A (1946) On the recrystallization of amorphous cellulose. J Am Chem Soc 68:2547–2552

Hesse S, Jaeger C (2005) Determination of the ^{13}C chemical shift anisotropies of cellulose I and cellulose II. Cellulose 12:5–14

Hesse S, Kondo T (2005) Behavior of cellulose production of *Acetobacter xylinum* in ^{13}C-enriched cultivation media including movements on nematic ordered cellulose templates. Carbohydr Polym 60(4):457–465

Hesse-Ertelt S, Witter R, Ulrich AS, Kondo T, Heinze T (2008) Spectral assignments and anisotropy data of cellulose I_α: ^{13}C-NMR chemical shift data of cellulose I_α determined by INADEQUATE and RAI techniques applied to uniformly ^{13}C-labeled bacterial celluloses of different *Gluconacetobacter xylinus* strains. Magn Reson Chem 46:1030–1036

Hestrin S, Schramm M (1954) Synthesis of cellulose by *Acetobacter xylinum*. 2. Preparation of freeze dried cells capable of polymerizing glucose to cellulose. Biochem J 58:345–352

Hirai A, Tsuji M, Horii F (1997) Culture conditions producing structure entities composed of cellulose I and II in bacterial cellulose. Cellulose 4:239–245

Jayme G, Knolle H (1964) The empirical X-ray determination of the degree of crystallinity of cellulosic material. Papier 18:249–255

Kai A, Arashida T, Hatanaka K, Akaike T, Matsuzaki K, Mimura T, Kaneko Y (1994) Analysis of the biosynthetic process of cellulose and curdlan using ^{13}C-labeled glucose. Carbohydr Polym 23:235–239

Kai A, Karasawa H, Kikawa M, Hatanaka K, Matsuzaki K, Mimura T, Kaneko Y (1998) Biosynthesis of ^{13}C-labeled branched polysaccharides by pestalotiopsis from ^{13}C-labeled glucoses and the mechanism of formation. Carbohydr Polym 35:271–278

Kast W, Flaschner L (1948) Eine röntgenographische Methode zur Bestimmung des Verhältnisses von kristalliner und amorpher Substanz in Zellulosefasern. Coll Polym Sci 111(1):6–15

Klemm D, Schumann D, Udhardt U, Marsch S (2001) Bacterial synthesized cellulose—artificial blood vessels for microsurgery. Prog Polym Sci 26:1561–1603

Klemm D, Heublein B, Fink HP, Bohn A (2005) Cellulose: Fascinating biopolymer and sustainable raw material. Angew Chem Int Ed 44:3358–3393

Kondo T, Togawa E, Brown RM Jr (2001) Nematic ordered cellulose: a concept of glucan chain association. Biomacromolecules 2:1324–1330

Kondo T, Nojiri M, Hishikawa Y, Togawa E, Romanovicz D, Brown RM Jr (2002) Biodirected epitaxial nanodeposition

of polymers on oriented macromolecular templates. Proc Natl Acad Sci USA 99:14008–14013

Kono H, Numata Y (2006) Structural investigation of cellulose I_α and I_β by 2D RFDR NMR spectroscopy: determination of sequence of magnetically inequivalent D-glucose units along cellulose chain. Cellulose 13:317–326

Kono H, Yunoki S, Shikano T, Fujiwara M, Erata T, Takai MJ (2002) CP/MAS ^{13}C NMR study of cellulose and cellulose derivatives. 1. Complete assignment of the CP/MAS ^{13}C NMR spectrum of the native cellulose. Am Chem Soc 124:7506–7511

Kono H, Erata T, Takai M (2003) Determination of the through-bond carbon–carbon and carbon-proton connectivities of the native celluloses in the solid state. Macromolecules 36:5131–5138

Kuga S, Brown RM Jr (1991) Physical structure of cellulose microfibrils: Implication for biogenesis. In: Haigler CH, Weimer PJ (eds) Biosynthesis and biodegradation of cellulose. M. Dekker, Inc, New York, Basel, Hong Kong, p VI/125ff

Kuga S, Takagi S, Brown RM Jr (1993) Native folded-chain cellulose II. Polymer 34:3293–3297

Meyer KH, Misch L (1937) Position des atomes dans le nouveau module spatial de la cellulose. Helv chim Acta 20:232–244

Numata Y, Kono H, Kawano S, Erata T, Takai M (2003) Cross-polarization/magic-angle spinning ^{13}C nuclear magnetic resonance study of cellulose I–ethylenediamine complex. J Biosci Bioeng 96:461–466

Sarko A, Muggli R (1974) Packing analysis of carbohydrates and polysaccharides. III. Valonia cellulose and cellulose II. Macromolecules 7:486–494

Schenzel K, Fischer S (2001) NIR FT Raman spectroscopy–a rapid analytical tool for detecting the transformation of cellulose polymorphs. Cellulose 8:49–57

Schenzel K, Fischer S, Brendler E (2005) New method for determining the degree of cellulose I crystallinity by means of FT Raman spectroscopy. Cellulose 12:223–231

Seifert M, Hesse S, Kabrelian V, Klemm D (2004) Controlling the water content of never dried and reswollen bacterial cellulose by the addition of water-soluble polymers to the culture medium. J Polym Sci A (Chem) 42:463–470

Togawa E, Kondo T (1999) Change of morphological properties in drawing water-swollen cellulose films prepared from organic solutions: a view of molecular orientation in the drawing process. J Polym Sci B (Phys) 37:451–459

Udhardt U, Hesse S, Klemm D (2005) Analytical investigations of bacterial cellulose. Macromol Symp 223:201–212

VanderHart DL, Atalla RH (1984) Studies of microstructure in native celluloses using solid state ^{13}C NMR. Macromolecules 17:1465–1472

Watanabe K, Tabuchi M, Morinaga Y, Yoshinaga F (1998) Structural features and properties of bacterial cellulose produced in agitated culture. Cellulose 5:187–200

Wiley JH, Atalla RH (1987) Bands assignments in the Raman spectra of celluloses. Carbohydr Res 160:113–129